Title

DNA double-strand break movement in heterochromatin depends on the histone acetyltransferase dGcn5.

Journal

Nucleic Acids Research, 52(19)

Authors

Kendek, Apfrida
Sandron, Arianna
Lambooij, Jan-Paul
et al.

Publication Date

2024-10-28

DOI

10.1093/nar/gkae775

Peer reviewed

Nucleic Acids Research, 2024, **52**, 11753–11767
https://doi.org/10.1093/nar/gkae775
Advance access publication date: 11 September 2024
Genome integrity, repair and replication

DNA double-strand break movement in heterochromatin depends on the histone acetyltransferase dGcn5

Apfrida Kendek[1,†], Arianna Sandron[1,†], Jan-Paul Lambooij[1], Serafin U. Colmenares[2], Severina M. Pociunaite[1], Iris Gooijers[1], Lars de Groot[1], Gary H. Karpen[2,3] and Aniek Janssen[1,*]

[1]Center for Molecular Medicine, University Medical Center Utrecht, Universiteitsweg 100, 3584 CG, Utrecht, the Netherlands
[2]Department of Molecular and Cell Biology, University of California, Berkeley, CA 94720, Berkeley, California, USA
[3]Division of Biological Sciences and the Environment, Lawrence Berkeley National Laboratory, CA 94720, Berkeley, California, USA

[*]To whom correspondence should be addressed. Tel: +31 887550701; Email: a.janssen-2@umcutrecht.nl
[†]The first two authors should be regarded as Joint First Authors.

Abstract

Cells employ diverse strategies to repair double-strand breaks (DSBs), a dangerous form of DNA damage that threatens genome integrity. Eukaryotic nuclei consist of different chromatin environments, each displaying distinct molecular and biophysical properties that can significantly influence the DSB-repair process. DSBs arising in the compact and silenced heterochromatin domains have been found to move to the heterochromatin periphery in mouse and *Drosophila* to prevent aberrant recombination events. However, it is poorly understood how chromatin components, such as histone post-translational modifications, contribute to these DSB movements within heterochromatin. Using irradiation as well as locus-specific DSB induction in *Drosophila* tissues and cultured cells, we find enrichment of histone H3 lysine 9 acetylation (H3K9ac) at DSBs in heterochromatin but not euchromatin. We find this increase is mediated by the histone acetyltransferase dGcn5, which rapidly localizes to heterochromatic DSBs. Moreover, we demonstrate that in the absence of dGcn5, heterochromatic DSBs display impaired recruitment of the SUMO E3 ligase Nse2/Qjt and fail to relocate to the heterochromatin periphery to complete repair. In summary, our results reveal a previously unidentified role for dGcn5 and H3K9ac in heterochromatic DSB repair and underscore the importance of differential chromatin responses at heterochromatic and euchromatic DSBs to promote safe repair.

Graphical abstract

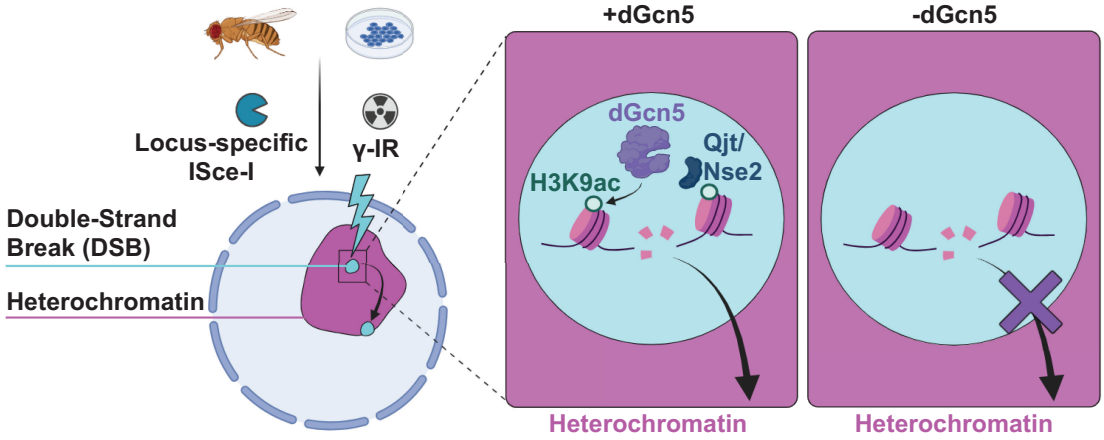

Introduction

DNA double-strand breaks (DSBs), in which both strands of the DNA helix are severed, are one of the most harmful lesions known to occur in genomes. DSBs can be caused by both exogenous and endogenous sources, and when repaired improperly can directly result in the formation of aberrant chromosome structures linked to genetic diseases and cancer (1–4). The two main DSB repair pathways in eukaryotic cells are homologous recombination (HR) and non-homologous end-joining (NHEJ). HR requires 5′ to 3′ end-resection at the DSB site, which results in a single-stranded 3′ DNA end that invades and perfectly copies a homologous sequence to safely repair the DSB. In contrast, NHEJ involves simple ligation of the DSB ends, but often results in small nucleotide insertions or deletions at the repaired site (5,6).

How different chromatin environments influence the cellular response to DSBs is less well understood (7). Eukaryotic nuclei can be roughly subdivided into two types of chromatin: euchromatin, which is characterized by a more open conformation and contains most of the transcriptionally

Received: March 26, 2024. **Revised:** August 20, 2024. **Editorial Decision:** August 22, 2024. **Accepted:** August 26, 2024

active protein-coding genes, and heterochromatin, which is more compact and relatively gene poor. Constitutive heterochromatin is one of the most prominent types of heterochromatin and is enriched at pericentromeric and subtelomeric regions. It contains highly repetitive DNA sequences, which are enriched for histone H3 Lysine 9 di- and tri-methylation (H3K9me2/3) and its epigenetic reader protein Heterochromatin Protein 1a (HP1a in *Drosophila*, HP1α in mammals) (8–13). Moreover, constitutive heterochromatin often coalesces into one or a few cytologically distinct domains in interphase nuclei (14,15), which represent biocondensates that form through the specific biophysical properties of HP1a (16,17).

The compacted nature of heterochromatin influences the response to DSBs arising in this compartment. It has been previously found that efficient repair in heterochromatin requires a chromatin reorganization step through the displacement of several core components, such as HP1β and KRAB-associated protein-1 (Kap1), which are respectively phosphorylated by ataxia telangiectasia mutated (ATM) and casein kinase 2 (CK2) upon damage induction (18–24). These events are thought to promote heterochromatin relaxation, thus overcoming the physical barrier imposed by heterochromatin and allowing DSB repair. In line with this, chromatin decompaction has been observed at damaged pericentromeric heterochromatin (PCH) in different species (25–28).

Moreover, the highly repetitive sequence content within PCH makes this domain especially vulnerable to erroneous recombination events between homologous sequences present on non-homologous chromosomes. Previous work in *Drosophila* and mouse has revealed that heterochromatic DSBs can undergo end-resection within the PCH domain, but only complete HR once relocated to the heterochromatin- or nuclear-periphery (25,28–30). This DSB movement is thought to prevent aberrant HR repair within the repeat-rich heterochromatin domain (25,31).

Several proteins have been found to be rapidly recruited to heterochromatic DSBs and promote DSB movement and HR repair. These include the structural maintenance of chromosomes 5/6 (SMC5/6) complex and the associated Nse2 SUMO E3 ligase (25,29,32). SMC5/6, as well as the other two SMC complexes cohesin and condensin, are conserved throughout the kingdoms of life (33). The characteristic ring shape of SMC complexes enables them to bring multiple DNA sequences into close proximity and thereby play a crucial role in genome folding and organization (33–35). SMC5/6 is known to promote genome stability in various pathways including chromosome segregation (36,37), telomere maintenance (38) and DNA damage repair (39–42). More specifically, the recruitment of SMC5/6 and its SUMO E3 ligase subunit Nse2 [Cervantes (Cerv) and Quijote (Qjt) in *Drosophila*] to heterochromatic DSBs is thought to mediate the SUMOylation of target proteins and in turn facilitate heterochromatic DSB movement through downstream signaling cascades (29,32).

Although many histone modifications have been identified at euchromatic DSB sites (43,44), histone changes at heterochromatic DSBs remain poorly understood. However, the distinct molecular and biophysical properties of heterochromatin suggest that DSB repair in this compact region requires specialized chromatin changes to allow DSB movement and repair protein recruitment. For example, we previously showed that the histone demethylase *Drosophila* KDM4A (dKDM4A) specifically promotes the demethylation of H3K9me2/3 and H3K56me2/3 at heterochromatic DSB sites, and is required for their movement and repair pathway choice (45,46). Whether this demethylation is accompanied by additional changes in heterochromatin composition remains untested.

In budding yeast and mammalian cells, the acetylation of histone H3 Lysine 9 (H3K9ac) by the histone acetyltransferase General Control Non-repressed protein 5 (GCN5, dGcn5 in *Drosophila*) is involved in several types of DNA damage repair, such as UV-damage (47), oxidative damage (48), and DSBs (49,50). While one study reported that loss of GCN5 results in a decrease in H3K9ac levels in cells following damage induction (48), other studies observed increases (47,49,50). However, these studies did not distinguish the responses in different pre-existing chromatin environments. It thus remains to be tested whether different chromatin environments, in particular the dense constitutive heterochromatin domain, differentially depend on H3K9ac for repair of damaged sites.

Using irradiationt of *Drosophila* tissues and cells in culture, as well as our previously established *in vivo* single-DSB (DR-*white*) system in *Drosophila* tissues (30), here we identify a specific increase in H3K9ac at heterochromatic DSBs. This H3K9ac is dependent on the histone acetyl transferase dGcn5, which is rapidly recruited to DSBs within the heterochromatin domain. Moreover, loss of dGcn5 results in defective DSB movement, as well as impaired recruitment of the SUMO E3 ligase Nse2/Qjt to heterochromatic DSBs. Together, our results identify a previously unrecognized role for dGcn5 and H3K9ac in the movement and repair of DSBs within the compact heterochromatin domain.

Materials and methods

Constructs

ATRIP, Qjt, dGcn5, elp3, Mu2 and HP1a were each cloned from cDNA generated from wild type Oregon-R adult flies. cDNA for each gene was cloned into a pCopia plasmid backbone containing an N-terminal fluorescent tag (CFP, YFP, GFP or mCherry).

Fly lines and genetic assays

All fly lines were reared at 22°C in standard medium unless otherwise stated. DR-*white* fly lines have been previously described (30). Heterozygous dGcn5 [E333st]/+ flies were obtained from the Bloomington *Drosophila* Stock Center (#9333) and the mei41 [29D] mutant line was kindly provided by Tin Tin Su. The ΔdKDM4A [KG04636] deletion mutant was kindly provided by Mattias Mannervik (51). The viability percentage of dGcn5 mutants was calculated using the ratio of adult males heterozygous for dGcn5 [E333st] compared to wild type offspring. The viability percentage of ATR and dGcn5 double mutants was calculated using the ratio of adult males hemizygous for mei41 [29D] and heterozygous for dGcn5 [E333st] compared to males hemizygous for mei41 [D29] and wildtype for dGcn5. Mei41 [29D] resides on the X chromosome and hemizygous mutant males without exogenous DNA damage do not have significant viability problems (52).

Chromatin immunoprecipitation-quantitative PCR (ChIP-qPCR)

Third instar larvae from DR-*white* fly lines containing the *hsp.I-SceI* transgene were heat-shocked at 37°C for 1 h and snap-frozen in liquid nitrogen 6 h after heat-shock treatment. Larvae from DR-*white* fly lines not containing the *hsp.I-SceI* transgene were used as controls and subjected to the same heat-shock treatment. Frozen larvae were stored at −80°C until chromatin extract preparation. For chromatin extract preparation, 80 larvae per line were homogenized, fixed and sonicated as described within the modENCODE project (https://www.encodeproject.org/documents/f890fde6-924c-4265-a60f-c5810401066d/, ChIP protocol by Kevin White lab) (53). ChIP procedures were performed on chromatin extracts as previously described (54). Each ChIP sample was prepared with 2 μg of chromatin extract and 5 μg of anti-H3K9ac antibody. For the γH2Av ChIP, 2 μg of chromatin and 20 μl of anti-γH2Av antibody were used. qPCR was used to quantify the enrichment levels of histone marks of interest using the qPCR FastStart Universal SYBR Green Master Mix (Roche) and qPCR specific primers targeting the I-SceI site (*3xp3*) or the *yellow* gene as a control (Supplementary Table S1).

Cell culture, dsRNA production and transfection

S2 and Kc167 (Kc) cells were cultured at 27°C in Schneider's insect medium (Sigma-Aldrich) containing 10% FBS and CCM3 serum-free medium (HyClone) respectively. For RNAi experiments, dsRNA was generated by first adding a T7-promoter sequence to the region of interest via PCR, followed by reverse transcription using the MEGAScript T7 transcription kit (Life Technologies) according to the manufacturer's instructions (Supplementary Table S1). 5-10 μg of dsRNA were used to transfect 200 000 cells 5 days prior to irradiation. As a control, dsRNA targeting the *yellow* gene was always included. For live imaging experiments, cells were transfected with fluorescent proteins of interest approximately 6 h prior to dsRNA transfection. For live imaging of Qjt, Kc cells were transfected with GFP-Qjt and Hygromycin resistance plasmids. Cells were selected for 2 weeks using 200 μg/ml Hygromycin to generate Kc cells with stable GFP-Qjt expression. All transfections were performed using TransIT-2020 transfection reagent (Mirus) according to the supplier's manual.

γ-Ray irradiation

Irradiation was performed by exposing cells to 5 Gy (0.0289 Gy/s) of γ-rays in an IBL 437C machine at 22°C. The source of γ-rays is 137-Cs decay.

Reverse transcription-quantitative PCR (RT-qPCR)

Knock down efficiency was verified by reverse transcription-quantitative polymerase chain reaction (RT-qPCR). Cells transfected with dsRNA were harvested after 5 days and RNA was extracted using the RNeasy Micro Kit (Qiagen) according to the manufacturer's instructions. cDNA was obtained by using the iScript cDNA synthesis kit (BioRad). RT-qPCR reaction, using cDNA as template, was performed on a thermocycler using primers targeting *tubulin* as control. To test mRNA levels in dGcn5 [E333st] larvae, RNA extraction and RT-qPCR were conducted as previously described (46) (see Supplementary Table S1 for primers used).

Immunofluorescence (IF) and EdU staining

For IF staining on cells in culture, fixation was achieved by incubating cells with 4% paraformaldehyde (PFA) in PBS for 5 min. Next, cells were incubated with 0.4% Triton-X diluted in PBS for 10 min to allow for permeabilization. Blocking was subsequentially performed by adding 5% milk, 0.4% Triton-X diluted in PBS for 1 h. Primary antibodies were incubated overnight at 4°C, followed by secondary antibody and DAPI incubation for 2 h at room temperature, all diluted in blocking solution. Finally, cells were mounted on glass slides using ProLong Diamond Antifade Mountant (Invitrogen). For IF staining of tissue, wing discs were dissected from third instar larvae in 10 μl of Schneider's Insect Medium containing 10% FBS and fixed on a glass slide with 4% PFA for 5 min. Slides were dipped in liquid nitrogen and stored at -20°C in 99% ethanol. Slides were brought to room temperature, incubated in PBS for 20 min and subsequently blocked in 5% milk, 0.4% Triton-X diluted in PBS for 1.5 h. The following steps (primary and secondary antibodies incubation, mounting on glass slide) were performed as described above for fixed cells. For EdU staining, Kc cells were incubated with 10 μM EdU for 30 min. EdU detection was performed according to Click-iT EdU Imaging Kits Protocol (Invitrogen).

Antibodies and dilutions

For ChIP-qPCR, experiments were performed with the anti-H3K9ac (Epicypher 13-0020, 13-0033) antibody and the anti-γH2Av (Hybridoma Bank, UNC93-5.2.1) antibody. For IF experiments on tissues and cells, the following primary antibodies were used: anti-H3K9ac (rabbit, Epicypher 13-0033, 1:500), anti-γH2Av (mouse, Hybridoma Bank, UNC93-5.2.1, 1:250), FlexAble Coralite Plus 555 conjugated anti-H3K9me3 (rabbit, ab8898, 1:500). The following secondary antibodies were used: Alexa goat anti-rabbit 488 (1:600), Alexa goat anti-mouse 568 (1:600) (Invitrogen).

Imaging and quantifications

Images were acquired using a widefield fluorescence microscope (DeltaVision Spectris, Applied Precision, LLC) using a 60× oil immersion objective (NA 1.40). For live imaging experiments, Z-stack images (22 slices with 0.5 μm Z spacing) were acquired every 10 min. Deconvolution was performed using the SoftWoRx (Applied Precision, LLC) software with the following parameters: deconvolution method was set as 'conservative' and the number of processing cycles used was seven. Image analysis was manually performed on deconvoluted images using Fiji software. For Figure 1E, F, quantification of H3K9ac intensity levels was performed as follows: for non-irradiated cells, regions of interest (ROIs) were manually drawn around the H3K9me3-weak regions (euchromatin) and H3K9me3-rich regions (heterochromatin) of each cell and the mean H3K9ac intensity was measured therein. Since Z-stacks (40 slices of 0.2 μm distances) were acquired during imaging, for each cell the quantification was conducted on the Z section displaying the most intense and focused H3K9me3 signal. For irradiated cells, γH2Av foci were used to identify DSBs, and H3K9me3 staining was used to determine euchromatin (low intensity H3K9me3 signal) and heterochromatin (high intensity H3K9me3 signal). Only cells displaying at least one

DSB in heterochromatin were included in the analysis. In some cells, after damage induction small H3K9me3-high foci can be found to localize inside the H3K9ac-high region of the cells (which indicates euchromatin); these H3K9me3-high regions were excluded from quantification, since it has been reported that H3K9me3 could be newly deposited at euchromatic DSBs (55). A region of interest was drawn around DSBs in euchromatin and heterochromatin and the H3K9ac intensity inside the regions was measured. Finally, the H3K9ac background signal (intensity of H3K9ac outside cells) was subtracted from the measurements.

RNA-sequencing procedure

Kc cells were depleted of dGcn5 or yellow (control) for 5 days using dsRNA as described above. Cells were harvested and RNA was isolated using the RNeasy Micro Kit (Qiagen). The quality and quantity of the RNA samples was measured using the Agilent Fragment Analyzer 5300 system and Qubit (Invitrogen) respectively. 100 ng of total RNA was used to prepare TruSeq Stranded mRNA libraries (20020594) following the manufacturer's protocol with custom 384 xGen UDI-UMI adapters (IDT). Prepared libraries were validated with the Fragment Analyzer system dsDNA 910 Reagent Kit (35-1500 bp) and Qubit dsDNA HS Assay Kit (Cat. Q32854). All libraries were then pooled in equimolar ratio and sequenced on a Nextseq2000 (Illumina) by using a P2 flow cell with 50 bp paired-end reads.

RNA-sequencing data analysis

Quality control on the sequence reads from the raw FASTQ files was performed with FastQC (v0.11.8). TrimGalore (v0.6.5) was used to trim reads based on quality and adapter presence after which FastQC was again used to check the resulting quality. rRNA reads were filtered out using SortMeRNA (v4.3.3) followed by alignment to the reference genome fasta (Drosophila_melanogaster. BDGP6.32) using the STAR (v2.7.3a) aligner. Follow-up QC on the mapped (bam) files was performed using Sambamba (v0.7.0), RSeQC (v3.0.1) and PreSeq (v2.0.3). Readcounts were then generated using the Subread FeatureCounts module (v2.0.0) with the Drosophila_melanogaster.BDGP6.32.105.chr.gtf file as annotation. CPM and RPKM Normalized versions of the counts table were generated using the R-packages edgeR (v3.28) as well as a normalized version using DEseq2 (v1.28). The differential expression analysis was performed using DESeq2.

Statistics and graphs

All statistical analysis were performed in GraphPad Prism. Plots were generated in Python using Panda, Seaborn and matplotlib.

Results

The histone acetyl transferase dGcn5 deposits new H3K9ac marks at heterochromatic double-strand breaks

In order to gain insights into the influence of chromatin factors on the process of DSB repair in heterochromatin, we sought to determine changes in chromatin composition associated with heterochromatic DSBs. We previously observed demethylation of histone H3 Lysine 9 di- and tri-methylation (H3K9me2/me3) at heterochromatic DSBs (46). We hypothesized that additional chromatin changes, such as histone acetylation (26), could be required to overcome the compact heterochromatic state and promote DSB movement and repair. To test this, we employed our previously established DR-*white* single DSB system in *Drosophila* (Figure 1A) (30). In this system, the DR-*white* construct is integrated in a single euchromatic or pericentromeric heterochromatic (PCH) locus in the fly genome and contains an 18 base-pair recognition sequence targeted for DSB induction by the I-SceI endonuclease. To induce the expression of I-SceI and the consequent formation of DSBs, we heat-shocked third instar larvae containing one eu- or hetero-chromatic DR-*white* insertion as well as a heat-shock inducible I-SceI (*hsp.I-SceI*) transgene. ChIP-qPCR (Chromatin Immuno-precipitation (ChIP) followed by quantitative PCR (qPCR)) was performed on chromatin extracts upon I-SceI-dependent DSB induction (Figure 1B). Interestingly, we observed that the levels of the histone mark Histone H3 Lysine 9 acetylation (H3K9ac) increased at DSBs in three of the five heterochromatic DR-*white* lines (1.6–2.8-fold increase), whereas H3K9ac levels decreased or remained unchanged at three euchromatic insertion sites (Figure 1C, Supplementary Figure S1A). All DR-*white* loci were enriched for the DSB marker phosphorylated H2Av (γH2Av) following I-SceI expression, ruling out that differences in H3K9ac levels are due to variations in cutting efficiency (Supplementary Figure S1B–D). Importantly, internal controls demonstrate that the antibodies used in these experiments selectively bind H3K9ac nucleosomes (Supplementary Figure S2A, B).

Previous work by others in mammalian cells as well as budding yeast have reported both the accumulation and the reduction of H3K9ac levels at DNA damage sites (47–50). However, our ChIP-qPCR results indicate that increases in this histone mark are specific to DSBs in heterochromatin. This suggests that H3K9ac is differentially regulated in response to DSBs depending on the pre-existing chromatin domain.

It has been reported that H3K9ac deposition in *Drosophila* mainly depends on the histone acetyl transferase (HAT) dGcn5 and to a lesser extent on Elp3 (56–59). To assess which of these two HATs could be responsible for the acetylation of lysine 9 on histone H3 in *Drosophila*, we knocked down both proteins via RNA interference in *Drosophila* Kc cells (Supplementary Figure S2C, D), followed by immunofluorescence staining for H3K9ac. We find that depletion of dGcn5, but not Elp3, leads to decreased nuclear H3K9ac levels in undamaged cells, supporting the notion that dGcn5 represents the major acetyltransferase for H3K9ac in *Drosophila* (Supplementary Figure S2E, F) (60).

Next, to test whether dGcn5 or Elp3 are recruited to heterochromatic DSBs, we fluorescently tagged these proteins in *Drosophila* cells in culture. We combined their expression with fluorescently tagged HP1a (heterochromatin protein 1a) to visualize heterochromatin, and Mu2 (binds γH2Av, MDC1 homolog) to visualize DSBs. Strikingly, we observed co-localization of dGcn5 with DSBs (Mu2) in the HP1a domain within 5 min following 5 Gy ionizing radiation (IR) (Figure 1D), indicating that this HAT can be directly recruited to DSBs within heterochromatin. Consistent with previous observations, Elp3 localizes to the cytoplasm in undamaged cells (61), and this pattern was not affected by the induction of DSBs upon exposure to 5 Gy IR (Supplementary Figure S2G). Together, this suggests that dGcn5, but not Elp3, localizes to heterochromatic DSBs and represents the main H3K9ac

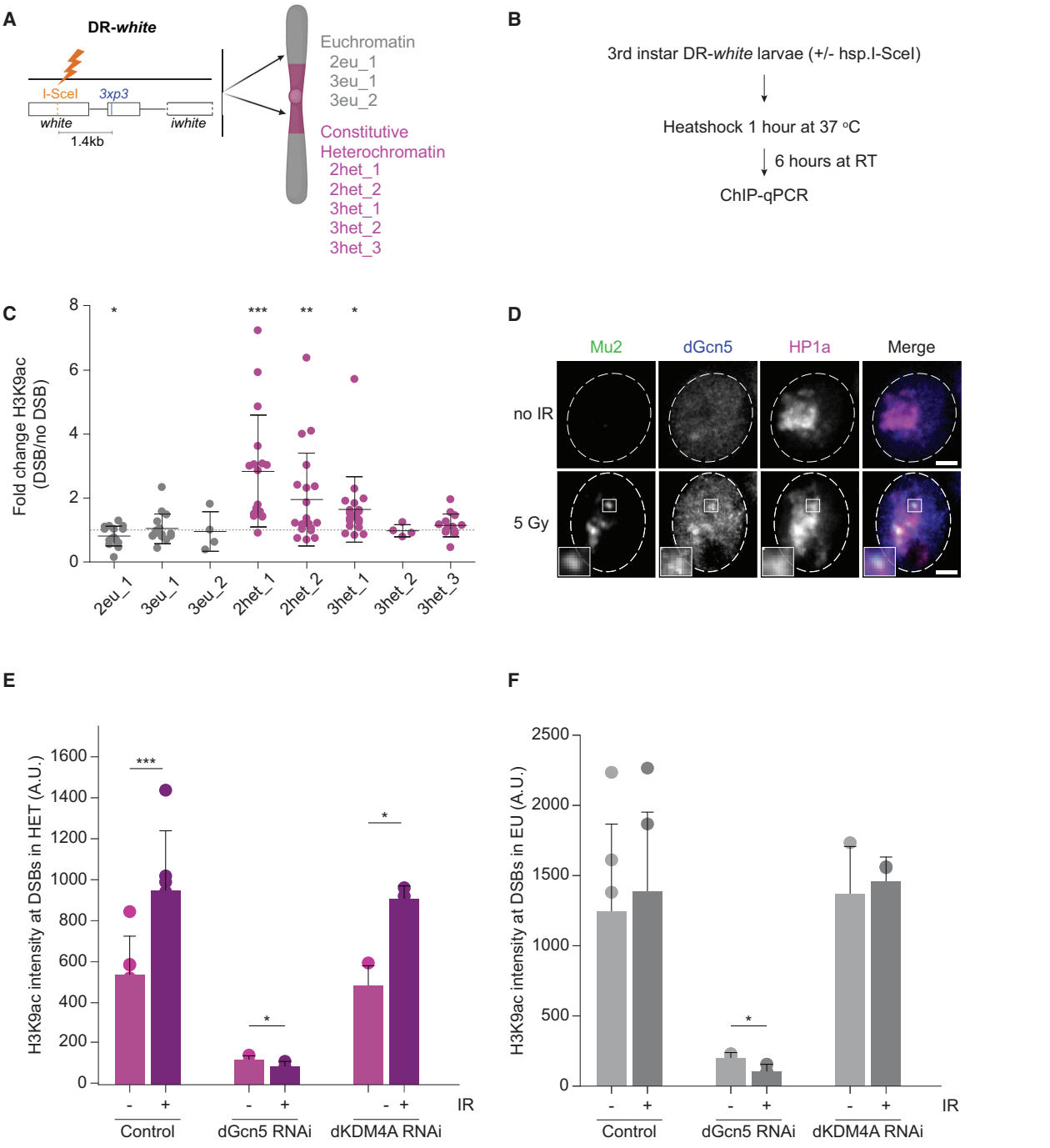

Figure 1. H3K9ac is increased at heterochromatic DSBs in a dGcn5-dependent manner. (**A**) Schematic representation of the DR-*white* system in *Drosophila*. The DR-*white* construct is integrated in a single euchromatic or heterochromatic locus in the fly genome to generate different lines (nomenclature as in (30)). The DR-*white* construct contains an 18-bp DNA sequence targeted by the I-SceI endonuclease, resulting in the formation of a single DSB (30). (**B**) Scheme detailing the DSB induction protocol in DR-*white* fly lines. Chromatin was extracted 6 h after DSB induction. DSBs were induced by a 1 h heat-shock (37°C) of third instar DR-*white* larvae containing a heat-shock promoter-driven I-SceI transgene (*hsp.I-SceI*). To control for heat-shock effects, all conditions (without/with *hsp.I-SceI*) are heat-shocked. (**C**) ChIP-qPCR analysis of H3K9ac levels at indicated DR-*white* loci. The qPCR primers reside 1.4 kb downstream of the I-SceI cut site ('*3xp3*' in Figure 1A). Fold change is calculated by dividing the H3K9ac enrichment levels in the damaged (+DSB, +I-SceI, Supplementary Figure S1A) samples by those in the controls (−DSB, no (−) I-SceI Supplementary Figure S1A). The grey dotted line represents a fold change of 1, in which H3K9ac levels are unchanged upon DSB induction. All qPCR results are relative to an internal control region (*yellow*), which is consistently enriched for H3K9ac. Error bars represent mean ± SD from ≥4 independent experiments. (**D**) Representative time-lapse images of non-irradiated (no IR) and irradiated (5 min after 5 Gy gamma-radiation) Kc cells with fluorescently tagged Mu2 (green, DSB marker), dGcn5 (blue) and HP1a (magenta, heterochromatin marker). Dashed lines outline the nuclei. Insets are zoom-in views of Mu2, dGcn5 and HP1a colocalization. Scale bar = 2 μm. (**E**, **F**) Quantification of H3K9ac intensity levels in heterochromatin (E, H3K9me3-enriched, immunofluorescence stainings performed as in Supplementary Figure S2H) and euchromatin (F, low H3K9me3, see Supplementary Figure S2H) at DSBs in non-irradiated versus irradiated control (*yellow* dsRNA), dGcn5-depleted and dKDM4A-depleted Kc cells. Irradiated cells were fixed 5-10 min after damage induction. Error bars represent mean + SD from ≥3 independent experiments. (*) *P*-value ≤ 0.05, (**) *P*-value ≤ 0.01, (***) *P*-value ≤ 0.001, paired *t*-test. If not shown, *P*-value not significant (>0.05). Figure 1A was created with Biorender.com.

transferase in *Drosophila* cells. We therefore focused our subsequent analyses on the potential role of dGcn5 at heterochromatic DSBs.

The observed localization of dGcn5 to DSBs in heterochromatin, and the general role for dGcn5 in H3K9ac (56) (Supplementary Figure S2E, F), led us to hypothesize that dGcn5 could be responsible for the observed increase in H3K9ac levels at heterochromatic DSBs (Figure 1C). Thus, we irradiated control and dGcn5-depleted cells and quantified the H3K9ac intensity levels in euchromatin (H3K9me3-low) and heterochromatin (H3K9me3-high) at DSBs (visualized by γH2Av) (Supplementary Figure S2H) 5 min after damage induction (Figure 1E). In line with our ChIP-qPCR results at single DSBs *in vivo* (Figure 1C), we find a significant increase in heterochromatic H3K9ac levels after irradiation of cells in culture (Figure 1E). In contrast, the H3K9ac increase was more modest and not significant in damaged euchromatic regions (Figure 1F). This result further supports the idea that H3K9ac levels are differentially regulated in damaged euchromatin and heterochromatin. Importantly, depletion of dGcn5 abolished the damage-dependent increase in H3K9ac levels, suggesting that dGcn5 is required for the deposition of new H3K9ac marks at the sites of heterochromatic DSBs (Figure 1E, F, Supplementary Figure S2H).

We previously found that the repair of heterochromatic DSBs depends on the removal of H3K9me2/3 by the demethylase dKDM4A (45,46). Since methylated histone residues are chemically resistant to other types of epigenetic modifications, we hypothesized that dKDM4A-mediated demethylation is necessary for the deposition of H3K9ac at heterochromatic DSBs. To test this, we irradiated control and dKDM4A-depleted cells and quantified the H3K9ac intensity levels at DSBs in euchromatin and heterochromatin (Supplementary Figure S3A, Figure 1E, F). Surprisingly, we found that the absence of dKDM4A did not affect the increase in H3K9ac levels at heterochromatic breaks. In line with our observations in cultured cells, we found that H3K9ac levels at heterochromatic DSBs were also unaffected in irradiated wing discs from homozygous dKDM4A mutant larvae (ΔdKDM4A) (Supplementary Figure S3B) (46,51). This suggests that the H3K9ac marks at DSBs in heterochromatin are not deposited on the same histones demethylated by dKDM4A, and therefore indicates that H3K9 demethylation and acetylation are two independent events occurring at heterochromatic DSBs.

In conclusion, our data reveal that the histone acetyl transferase dGcn5 is rapidly recruited to heterochromatic DSBs and deposits new H3K9ac marks at the damaged sites. Moreover, this heterochromatin-specific increase in H3K9ac occurs independently of dKDM4A-mediated H3K9me2/3 removal.

dGcn5 promotes timely movement and repair of heterochromatic DSBs

In *Drosophila*, heterochromatic DSBs relocate to the heterochromatin- and nuclear-periphery within 30 min after irradiation (25,29,30). Since we observed a heterochromatin-specific increase in dGcn5-mediated H3K9 acetylation as early as 5 min after irradiation (Figure 1D–F), we hypothesized that this local post-translational modification is one of the factors that promote heterochromatic DSB movement. To test this, we depleted dGcn5 in *Drosophila* cells in culture and assessed the presence of DSBs (γH2Av foci) in heterochromatin (DAPI bright (25,62)) and euchromatin (DAPI weak) at specific time points following 5 Gy irradiation (Figure 2A). Consistent with earlier findings (25), we find that the number of heterochromatic DSBs in control cells peaked 10-20 min after irradiation (Figure 2B). This peak was followed by a steep decrease in the number of γH2Av foci located within heterochromatin, indicative of DSB movement and repair (Figure 2B) (25). Cells depleted of dGcn5 acquired the same number of heterochromatic DSBs within a similar timeframe as control cells (Figure 2B). However, the number of DSBs remained high within the heterochromatin domain (30-180 min after irradiation) and did not decline as steeply as in control cells (Figure 2A, B). These results suggest that loss of dGcn5 results in delayed heterochromatic DSB movement when compared to the control. In euchromatin (DAPI weak), we did not observe any difference in number of DSBs between control and dGcn5 RNAi cells within 0-180 min after damage induction (Figure 2A, C).

Finally, we observed that 24 h after irradiation the number of heterochromatic DSBs in dGcn5-depleted cells was still significantly higher than in control cells, indicating that the absence of dGcn5 leads to persistent defects in DSB repair (Supplementary Figure S4A). We also observed persistent DSBs in euchromatin 24 h after irradiation, possibly reflecting an indirect effect of inefficient heterochromatic DSB repair (Supplementary Figure S4B). Altogether, our data indicate that knockdown of dGcn5 specifically results in impaired heterochromatic DSB movement.

Our results suggest that the demethylation of H3K9me3 by dKDM4A is not a pre-requisite for the dGcn5-mediated deposition of new H3K9ac marks at heterochromatic DSBs (Figure 1E, F). dGcn5 and dKDM4A might therefore be involved in two separate pathways that both promote DSB movement and repair in heterochromatin. In order to investigate this, we depleted dGcn5 and dKDM4A in *Drosophila* cells in culture and assessed the number of DSBs remaining in the heterochromatin domain 120 min after irradiation (Figure 2D, E, Supplementary Figure S4C, D). As previously reported by us (46), single depletion of dKDM4A led to an increase in DSB foci within heterochromatin, indicative of a defect in DSB movement (Figure 2D). Interestingly, simultaneous depletion of dGcn5 and dKDM4A led to an additive effect on the number of DSB foci remaining within heterochromatin when compared to their single depletions (Figure 2D). Moreover, the combined depletion of dGcn5 and dKDM4A did not cause an additive repair defect in euchromatin (Figure 2E). We conclude that the additive effect on heterochromatic DSB accumulation observed in dGcn5 and dKDM4A co-depleted cells suggests that H3K9ac and H3K9me2/3 demethylation are two independent histone modifying events that both promote heterochromatic DSB movement.

Previous studies found that heterochromatic DSB movement is predominantly associated with repair by HR (25,28). Early HR steps (e.g. end-resection) occur within heterochromatin, whereas the later steps of HR (i.e. Rad51 assembly) resume only after DSBs have moved outside of the heterochromatin domain (25). Since our data reveal a delayed heterochromatic DSB movement upon dGcn5 knockdown (Figure 2A, B), we wished to address whether the early HR process within the heterochromatin domain would be affected in the absence of dGcn5. ATR Interacting Protein (ATRIP) is one of the proteins involved in early HR repair by binding to the RPA-ssDNA complex (63) and has been found to be efficiently recruited to both eu- and hetero-chromatic DSBs (25,63). We

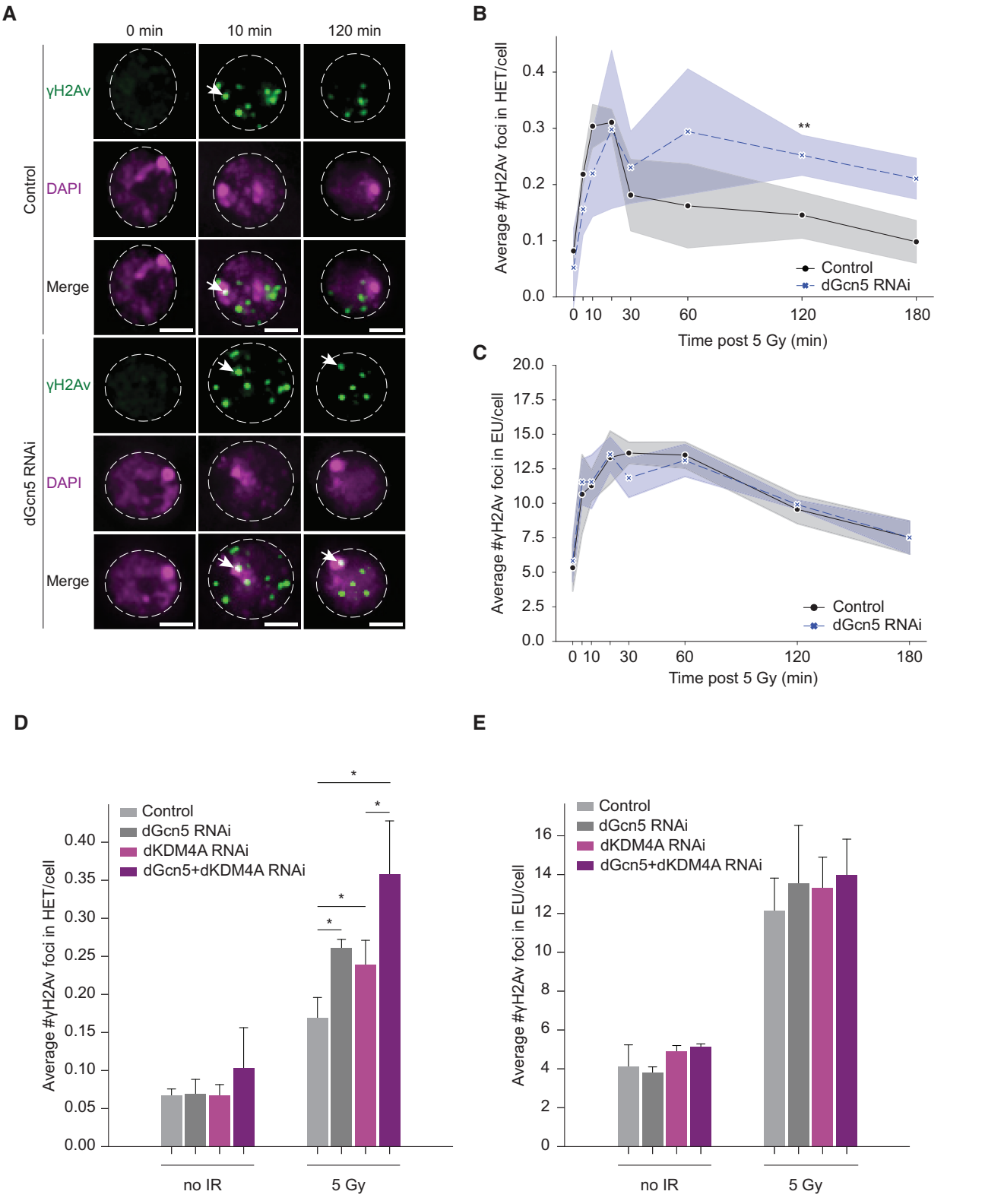

Figure 2. dGcn5 promotes repair of heterochromatic DSBs. (**A**) Representative images of Kc cells depleted for yellow (control) and dGcn5 fixed at indicated time points following 5 Gy irradiation. Cells were stained for γH2Av (green, DSB marker) and DAPI (magenta). White arrows indicate γH2Av foci in DAPI bright domain (heterochromatin). Dashed lines enclose the nuclei. Cells at time point 0 were fixed without prior irradiation. Scale bar = 2 μm. (**B**, **C**) Quantification of images as in (A). Average number of γH2Av foci in DAPI bright (B) and DAPI weak (C) is shown at indicated time points. Shade bars represent mean ± SD from three independent experiments. (**D**, **E**) Quantification of γH2Av foci inside DAPI bright (D) and DAPI weak (E) in non-irradiated versus 120 min after irradiation control (*yellow* dsRNA), dGcn5-depleted, dKDM4A-depleted or dGcn5 and dKDM4A co-depleted Kc cells. HET = heterochromatin, EU = euchromatin. Error bars represent mean + SD from three independent experiments. (*) *P*-value ≤ 0.05, (**) *P*-value ≤ 0.01, paired *t*-test. If not shown, *P*-value not significant (>0.05).

performed live imaging of fluorescently tagged ATRIP within the heterochromatin domain (visualized with HP1a) following 5 Gy irradiation in the absence and presence of dGcn5. By following ATRIP foci kinetics (time from appearance to disappearance) as well as its dynamics (movement) in the HP1a domain, we find that, in the absence of dGcn5, ATRIP foci in the HP1a domain display defective movement (Figure 3A–C). In the control situation, ATRIP foci remained on average 16 min in the HP1a domain (Figure 3C), after which they either move (52%, Supplementary Figure S4E) or get resolved within the domain. This is in line with previous live imaging of DSBs in fly tissues (30), which revealed that when DSBs arise inside the heterochromatic domain, they either move towards the heterochromatin periphery to complete repair or stay inside the domain and get resolved. These immobile DSBs represent a smaller percentage of damage foci and could potentially reflect repair by alternative mechanisms (e.g. NHEJ, MMEJ, SSA) (30).

When compared to control cells, ATRIP foci in dGcn5 depleted cells remained twice as long inside the HP1a domain (on average 41 min) before they moved out (32%, Supplementary Figure S4E) or resolved (Figure 3A–C). This result is consistent with the observed retention of γH2Av foci within heterochromatin in irradiated fixed cells (Figure 2). We do not find a defect in initial ATRIP recruitment to DSBs in heterochromatin (Supplementary Figure S4F), indicating that early end-resection steps can occur in the absence of dGcn5 and that, specifically, later steps (DSB movement and repair) are significantly delayed.

To exclude that the observed DSB repair defects are due to changes in expression of DSB repair genes, we performed bulk RNA-sequencing (RNA-seq) of dGcn5-depleted and control cells. These data reveal that the expression of known DSB repair genes remained unchanged upon dGcn5 depletion (Supplementary Figure S5A, Supplementary Tables S2 and S3). In addition, dGcn5 knockdown had no significant effect on the expression of cell-cycle regulated genes or cell-cycle progression based on RNA-seq data and EdU staining respectively (Supplementary Figure S5A, B, Supplementary Table S4).

Together, these results suggest that H3K9 acetylation, mediated by dGcn5, plays a crucial role in promoting the movement and HR repair of heterochromatic DSBs and functions independently of dKDM4A.

dGcn5 promotes the recruitment of the SUMO E3 ligase Nse2/Qjt to heterochromatic DSBs

Our results reveal that dGcn5 is required for the movement of heterochromatic DSBs (Figures 2 and 3), and therefore we sought to investigate the mechanism through which dGcn5 contributes to this process. One of the most important regulators of DSB movement in heterochromatin is *Drosophila* Nse2 (Cervantes/Quijote), a SUMO E3 ligase that is part of the SMC5/6 complex (32). In order to test the impact of loss of dGcn5 on *Drosophila* Nse2, we monitored the effect of dGcn5 depletion on the recruitment of Quijote (Qjt) to hetero- and eu-chromatic DSBs. We irradiated cells to induce the formation of DSBs and subsequently performed live imaging of fluorescently tagged Qjt and HP1a (Figure 4A–C). In line with previous studies (29,32), we find that Qjt overlaps with the complete heterochromatin domain (defined by HP1a) in non-irradiated cells, and that Qjt foci form in both eu- and hetero-chromatin upon irradiation (Figure 4A–C). These previous studies also showed that Qjt foci remain in the damaged heterochromatic domain until ∼10 min after DSB induction, then move outside of the domain (29,32). Interestingly, although we did not observe any difference in the appearance of γH2Av foci in heterochromatin 10 min after irradiation in control cells (Figure 2B), we do find that dGcn5-depleted cells display a decreased number of Qjt foci inside the HP1a domain (Figure 4B). Importantly, this phenotype was specific for Qjt recruitment to heterochromatic DSBs, as we observed no difference in the number of Qjt foci within euchromatin upon dGcn5 depletion (Figure 4C). This result suggests that dGcn5 promotes the recruitment of Qjt to heterochromatic DSBs, which is subsequently required for efficient and timely DSB movement outside the HP1a domain. Altogether, the DSB movement defects (Figures 2 and 3) and the impaired Qjt recruitment in dGcn5-depleted cells (Figure 4) suggest that dGcn5, and the dGcn5-dependent increase in H3K9ac at heterochromatic DSBs, act as key players in the DSB movement pathway in heterochromatin by stimulating the recruitment of crucial regulatory factors, such as Qjt, to the damaged heterochromatin domain.

dGcn5 mutant flies depend on ATR for their survival

In order to confirm the contribution of dGcn5 to heterochromatic DSB repair *in vivo*, we employed dGcn5 heterozygous mutant flies that contain a premature stop codon on residue 333 (dGcn5 [E333st]/+) (Figure 5A) (58). dGcn5 mutant flies are homozygous lethal but are heterozygous viable; heterozygous mutant larvae display a seventy percent reduction in dGcn5 mRNA and a significant decrease in H3K9ac levels (Supplementary Figure S6A–C) (58,64). We dissected wing discs tissues from dGcn5 [E333st]/+ third instar larvae and determined the number of DSBs (γH2Av foci) in heterochromatin (H3K9me3 region) before and after 5 Gy irradiation (Figure 5B, C). Consistent with our findings in cultured cells, we observed that, at 120 min after irradiation, DSBs accumulated in heterochromatin of dGcn5 mutant tissue, indicating that the movement of heterochromatic DSBs *in vivo* also requires dGcn5.

Finally, to assess the relevance of dGcn5-mediated H3K9 acetylation in living animals, we performed a synthetic lethality assay using dGcn5 [E333st]/+ flies. The DNA damage repair kinase Ataxia telangiectasia and Rad3 related (ATR) is one of the proteins that rapidly respond to DSB events (65). Moreover, ATR has been shown to promote heterochromatic DSB movement (25). Combining dGcn5 [E333st]/+ with an ATR truncation mutation (mei41 [29D]) (66) results in a 30% decreased viability (Figure 5D), highlighting the synergistic roles of dGcn5 and ATR in DSB repair. Altogether our results suggest that dGcn5 mutant synthetic lethality with ATR is due to compromised heterochromatic DSB movement and repair.

Discussion

Euchromatin and heterochromatin display different molecular and biophysical properties that can affect various aspects of DSB repair, including repair timing, DSB movement and repair pathway choice (31,44,67). While in recent years research has started to uncover the impact of chromatin components on DSB repair, much still remains to be discovered about how epigenetic changes at DSBs are orchestrated in

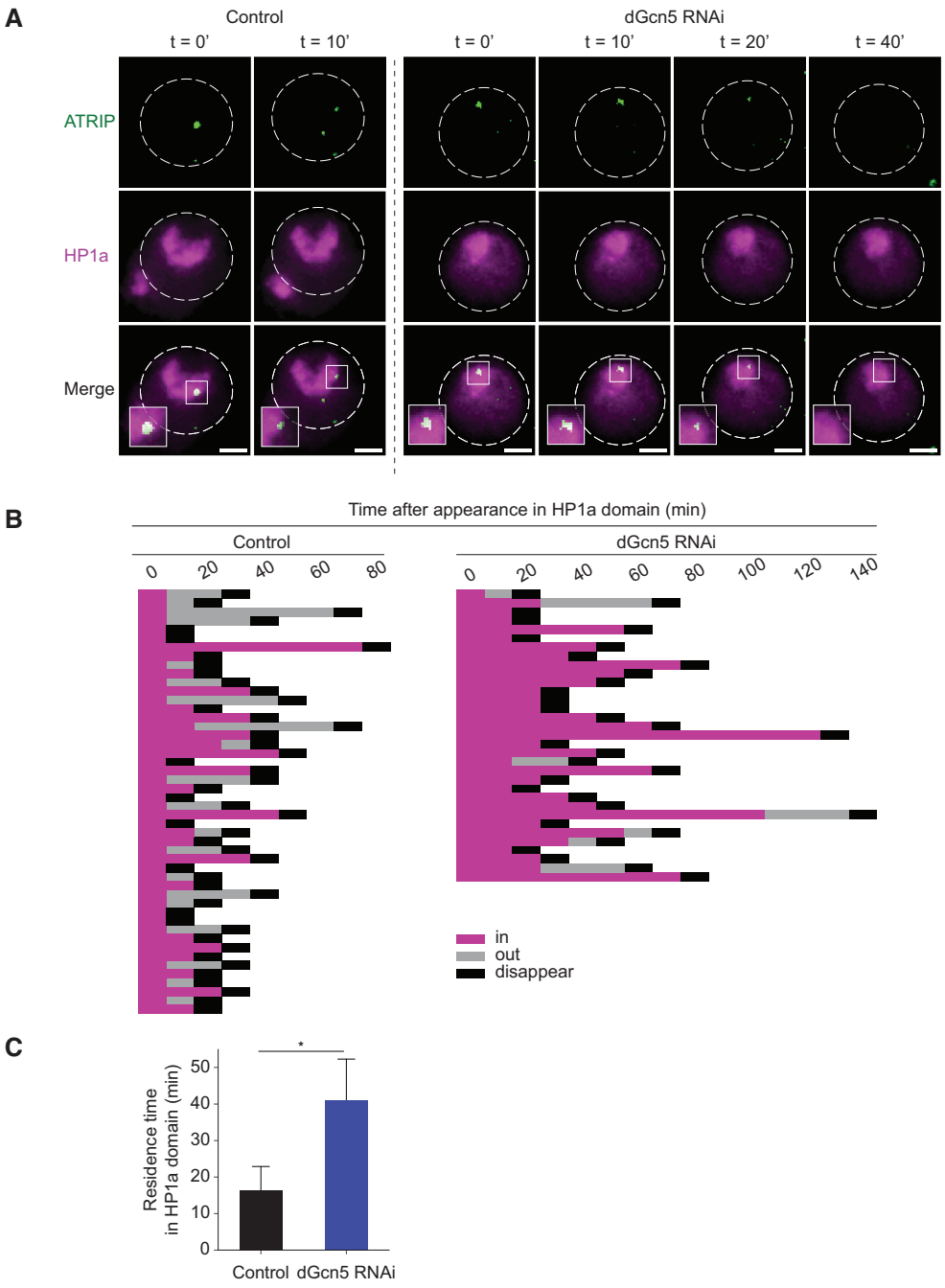

Figure 3. dGcn5 is required for DSB movement outside the HP1a domain. (**A**) Representative time-lapse images of ATRIP foci (green, HR protein) within the HP1a domain (magenta) in irradiated (5 Gy) control (*yellow* dsRNA) or dGcn5 depleted Kc cells. Insets are zoom-in views of heterochromatic ATRIP foci. Dashed lines enclose the nuclei. Scale bars = 2 μm. (**B**) Quantification of time-lapse movies as in (A). ATRIP foci movement and kinetics plotted from their appearance in the HP1a domain (0', magenta) to the timepoint they moved outside of the HP1a domain ('out', grey) or resolved ('disappear', black). Each row indicates quantification of one ATRIP focus. (**C**) Quantification of the mean residence time of ATRIP foci within the HP1a domain. (*) *P*-value ≤ 0.05, paired *t*-test. Error bars represent mean + SD from three independent experiments.

different pre-existing chromatin environments (31,44,67). Here, we find that the movement of DSBs outside the heterochromatin domain is accompanied by H3K9 acetylation to ensure efficient resolution of the damaged DNA. We used our previously developed inducible single-DSB system in *Drosophila* tissues (30), as well as irradiated *Drosophila* tissues and cultured cells to reveal that timely repair of heterochromatic DSBs depends on the dGcn5-mediated deposition of H3K9ac at the site of damage. In the absence of dGcn5, DSBs accumulate inside the HP1a domain and take twice as long to resolve or relocate outside heterochromatin (Figure 3). Moreover, we find that H3K9ac at heterochromatic DSBs occurs independently of H3K9me2/3 demethylation by dKDM4A, previously identified to be important for heterochromatic DSB movement and repair (46).

Our data further suggest that defective DSB movement upon dGcn5 loss results from inefficient recruitment of the SMC5/6 complex component Nse2/Qjt to heterochromatic

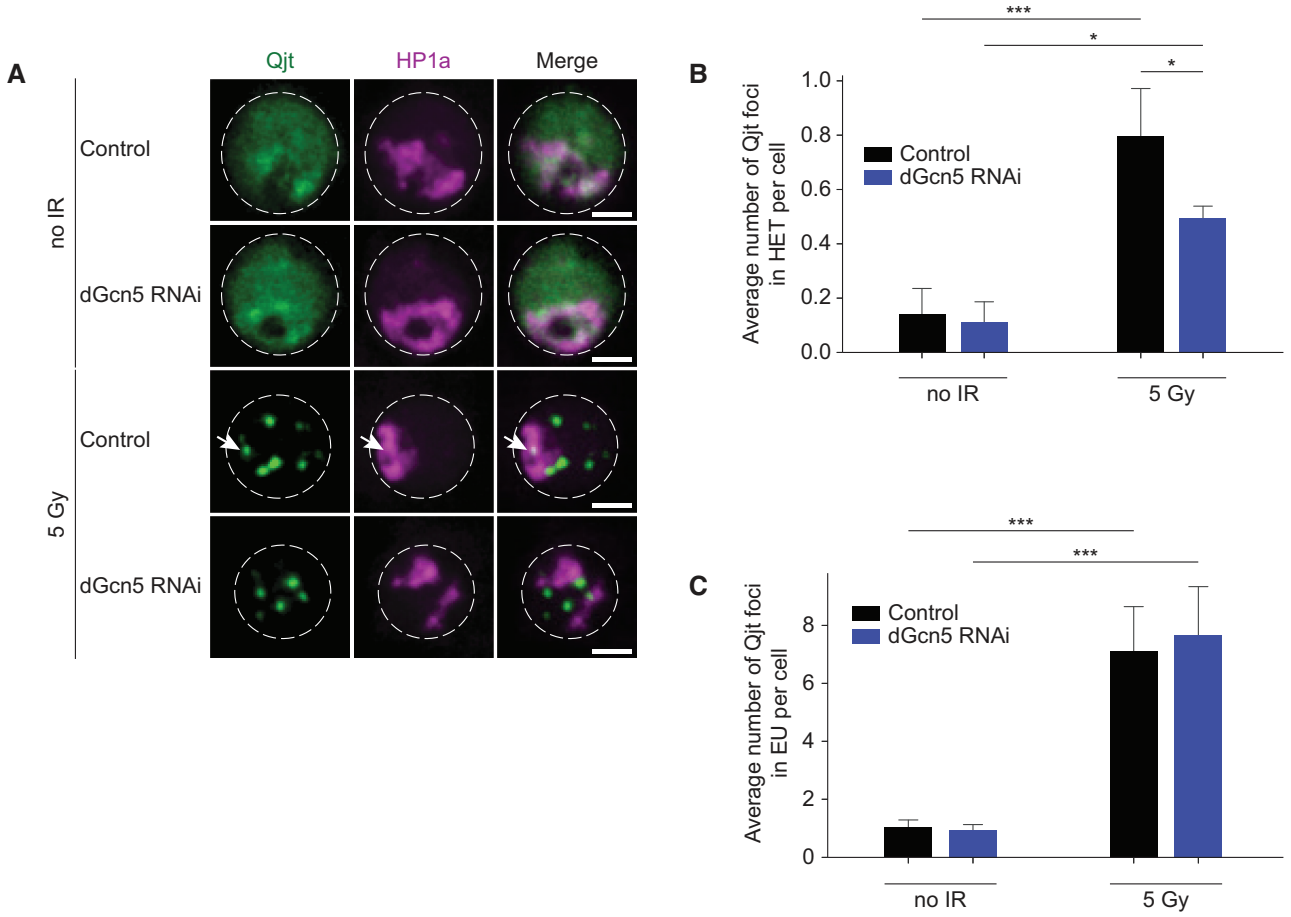

Figure 4. dGcn5 promotes Qjt recruitment at heterochromatic DSBs. (**A**) Representative time-lapse images of Kc cells expressing HP1a (magenta, heterochromatin) and Qjt (Nse2, green) with indicated conditions. Arrowhead indicates Qjt focus residing inside the HP1a domain. Dashed lines enclose the nuclei. Scale bars = 2 μm. (**B**, **C**) Quantification of Qjt foci inside the HP1a domain (B) and in euchromatin (C, outside HP1a domain) in non-irradiated versus 10 min after irradiation control (*yellow* dsRNA) and dGcn5-depleted Kc cells. HET = heterochromatin, EU = euchromatin. Error bars represent mean + SD from three independent experiments. (*) *P*-value ≤ 0.05, (***) *P*-value ≤ 0.001, one way ANOVA test followed by Tukey's multiple comparison. If not shown, *P*-value not significant (>0.05).

DSBs. We therefore propose a model in which dGcn5 mediates the local acetylation of heterochromatic H3K9 after DSB induction. Together with H3K9me2/3 demethylation, H3K9ac promotes movement and repair of the damaged DNA by facilitating the recruitment of Qjt to the HP1a domain (Figure 5E).

The finding that H3K9ac levels increase almost exclusively at DSB sites in pericentromeric heterochromatin (PCH) constitutes novel information. Indeed, previous work has reported both the accumulation and the reduction of H3K9ac at DNA damage sites in human and yeast cells (47–50). However, our *in vivo* ChIP-qPCR (Figure 1C) and cell data (Figure 1E, F) reveal that deposition of new H3K9ac marks is specifically enhanced at heterochromatic DSBs, suggesting that the levels of this mark are regulated according to the chromatin context in which the DSB is induced. This finding might therefore explain the conflicting results from previous studies in cells (47–50), which focused on the general chromatin response to DSBs, without considering differences in chromatin composition prior to DSB induction.

We found that two of the five DR-*white* heterochromatic lines (3het_2 and 3het_3) did not exhibit increase in H3K9ac levels at DSBs (Figure 1C), indicating that some degree of variability exists within the heterochromatin response to DSBs. We observed no correlation between the γH2Av- and the H3K9ac-fold change at DSB sites of different heterochromatic DR-*white* lines (Supplementary Figure S1, Figure 1), suggesting that the lack of H3K9ac enrichment at 3het_2 and 3het_3 DSBs is not caused by poor cutting efficiency of I-SceI. In addition, we previously found that the dKDM4A-dependent removal of H3K9me3 at the DR-*white* sites is efficient across all heterochromatic lines, indicating that the lack of newly-deposited H3K9ac at certain heterochromatic loci does not coincide with reduced removal of H3K9me2/3 (46). Lastly, we previously measured the levels of H3K9me3 at the undamaged DR-*white* heterochromatic loci through ChIP-qPCR (30) and found no correlation between the undamaged H3K9me3 levels and the post-damage H3K9ac levels across the DR-*white* heterochromatic lines, suggesting that the level of 'heterochromatinization' of a specific locus is not predictive of H3K9ac levels after damage induction.

Instead, our data suggest that different PCH regions may have differential H3K9ac dependencies for the repair of DSBs. For example, the necessity for H3K9ac at heterochromatic DSBs could potentially depend on the presence of other histone modifications or the localization of heterochromatic loci within the three-dimensional nucleus. These hypotheses could be tested in the future by examining the chromatin response to

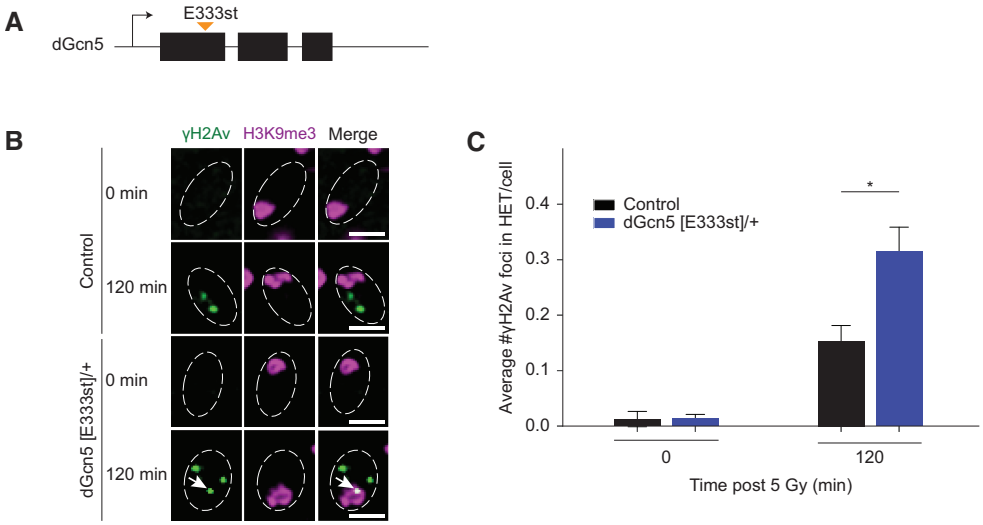

D

Genotype	Viability	N
Mei41+;dGcn5 [E333st]/TM3	0.68767	310
Mei41 [29D];dGcn5 [E333st]/TM3	0.48536	344
Relative viability of double mutant: 71% p-value 0.0004		

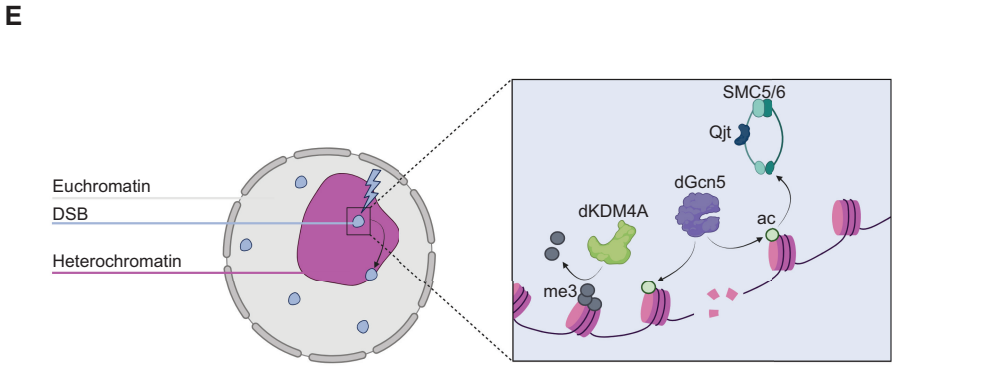

Figure 5. dGcn5 mutant is synthetically lethal with ATR mutant. (**A**) Schematic representation of the dGcn5 [E333st] mutation. dGcn5 consists of three exons (black rectangles) and two introns (lines in between the black rectangles). The premature stop codon (E333st, orange arrow in first exon) is introduced in the three nucleotides encoding for the 333rd amino acid (58). (**B**) Representative images of control and dGcn5 [E333st]/+ wing disc cells, fixed without prior irradiation (0 min) or 120 min after 5 Gy irradiation. Cells were stained for γH2Av (green, DSB marker) and H3K9me3 (magenta, heterochromatin marker). Dashed white lines indicate nuclei. Arrowheads indicate γH2Av foci inside the heterochromatic domain. Scale bar = 2 μm. (**C**) Quantification of images as in (B). Average number of γH2Av foci in heterochromatin is shown at indicated time points. Error bars represent mean + SD from three independent experiments. (*) *P*-value ≤ 0.05, one way ANOVA test followed by Tukey's multiple comparison. If not shown, *P*-value not significant (>0.05). (**D**) Synthetic lethality assay of dGcn5 mutant with ATR mutant. $N = 310$ flies for the control line (dGcn5 mutant, wild-type ATR allele (mei41+; dGcn5 [E333st]/+)) and $n = 344$ flies for the cross between dGcn5- and ATR- mutant flies (mei41 [29D]; dGcn5 [E333st]/+). Unpaired *t*-test. (**E**) Model for the role of dGcn5-mediated H3K9ac in heterochromatic DSB repair. The local transfer of an acetyl group onto H3K9 by dGcn5 at heterochromatic break sites leads to recruitment of SMC5/6-Nse2 (Qjt) which in turn promotes movement and repair of heterochromatic DSBs. The deposition of new H3K9ac marks by dGcn5 is independent of dKDM4A-mediated demethylation of H3K9me3. Figure 5E was created with Biorender.com.

DSBs induced at many different heterochromatic loci simultaneously, for example by adopting an approach similar to the one recently employed by Schep *et al.* (68,69).

Interestingly, we were able to observe dGcn5 localizing to DSB sites in heterochromatin, in line with previous *in vitro* and cell studies which reported dGcn5 being recruited to euchromatic DSBs and UV damage sites in both yeast and humans (47,49,50,70). The finding that dGcn5 localizes to heterochromatic DSBs and specifically promotes their movement opens up new research directions. For example, how is dGcn5 recruited to heterochromatic DSBs? Previously, we showed that movement and repair of heterochromatic DSBs in *Drosophila* depend on demethylation of H3K9me3 and H3K56me3 by the demethylase dKDM4A (45,46). It would therefore be tempting to hypothesize that dGcn5 recruitment depends on dKDM4A, which would conveniently allow for

control of H3K9ac deposition right after the demethylation of the same residue. However, in this study we find that the deposition of new H3K9ac marks by dGcn5 at heterochromatic DSBs does not require dKDM4A, suggesting that dGcn5 can be successfully recruited at break sites independently of dKDM4A. Several factors, including the MRN complex and the E2F1 transcription factor, have been previously implicated in promoting the localization of dGcn5 at euchromatic DNA damage sites in yeast and mammals (47,49,70). The recruitment of dGcn5 to heterochromatic DSBs might therefore depend on one of these proteins, although in this case another factor would have to confer specificity of the recruitment to heterochromatic DSBs.

We find that dGcn5 depletion leads to a decreased number of Qjt foci in damaged PCH, suggesting that dGcn5 or H3K9ac could also directly promote the recruitment of Qjt to DSBs. It has been previously reported that Qjt is recruited to heterochromatic DSBs as part of the SMC5/6 complex (25,29,32). Since none of the *Drosophila* SMC5/6 complex components possess a bromodomain (BRD, acetyl reader) (Uniprot database) (71), we hypothesize that the newly deposited H3K9ac marks do not act as direct binding sites for SMC5/6-Cerv/Qjt at DSBs. Nevertheless, one could envision a scenario in which Qjt is indirectly targeted by H3K9ac via an intermediate protein. Interestingly, a recent study in yeast proposed that dGcn5 and the SMC5/6 complex can directly interact, raising the possibility that the localization of Qjt at heterochromatic DSBs could also directly depend on dGcn5 binding (41).

While the SMC5/6 complex is also enriched at euchromatic DSBs (40), we did not observe a recruitment defect of Qjt to DSBs in euchromatin upon depletion of dGcn5 (Figure 4C). This suggests that Qjt binding to DSBs in eu- and heterochromatin is regulated through different pathways, where heterochromatic DSB recruitment of Qjt is promoted by dGcn5-mediated H3K9ac, while in euchromatin other pathways are involved. Finally, we and others observed that Qjt and the SMC5/6 complex are already broadly enriched in heterochromatin in undamaged conditions (25) (Figure 4A), and only become concentrated at specific DSB foci after irradiation. While the role of the SMC5/6 complex in unperturbed PCH is currently unknown, one intriguing possibility is that this localization pattern facilitates the fast recruitment of the complex to DSB sites upon deposition of new H3K9ac marks.

Another plausible role for H3K9ac at heterochromatic DSBs is the modulation of structural or biophysical properties of the damaged domain. dGcn5 has been reported to be important to promote chromatin accessibility at sites of DSBs and DNA replication (72,73). Moreover, H3K9ac is associated with transcription and therefore highly enriched in euchromatin (74–76). In the context of a biomolecular condensate such as heterochromatin (16,17), acetylation has been found to regulate the physical properties of chromatin by inhibiting phase separation (77). Therefore, the enrichment of H3K9ac at heterochromatic DSBs could stimulate the formation of a more open (euchromatin-like) structure, in order to facilitate DSB movement as well as the recruitment of certain repair factors. In line with this hypothesis, previous research has reported that heterochromatin decompaction at sites of DSBs is accompanied by accumulation of H4K5ac and removal of H3K9me3 (26). This raises the possibility that several 'permissive' histone marks, and not only H3K9ac, play important roles during the heterochromatic response to DSB and that, perhaps, the function of these newly-deposited marks is to collectively create a repair-permissive environment.

Interestingly, both H3K9me2/3 demethylation and H3K9 acetylation occur at DSBs in PCH. Although both histone modifying events are necessary for DSB movement, our results suggest these are two independent pathways. One intriguing possibility is that demethylation and acetylation independently change the biophysical properties of heterochromatin to allow repair. As such, demethylation could reduce the interaction of the DSB with HP1a and thereby locally promote the decompaction of the PCH domain. In addition, acetylation could make the chromatin state of the DSB incompatible with the heterochromatin domain, thereby promoting a more open, repair-permissive environment.

Interestingly, previous research in *Drosophila* revealed that a fraction of DSBs move from the heterochromatic core to the nuclear envelope, where repair is completed (29). While actin and myosin have been proposed to mediate the relocalization of DSBs between the heterochromatin periphery and the nuclear envelope, it is currently unknown what promotes the non-directed movement of DSBs from the inside to the periphery of the PCH domain (78). Our data suggest a possible mechanism for this step, where the demethylation and acetylation mediated by dKDM4A and dGcn5 respectively could alter the biophysical properties of the damaged DNA and thereby promote exclusion from the phase separated heterochromatin domain, thus triggering the relocalization of DSBs to the periphery of the domain. This is indeed in line with previous work that revealed histone acetylation can promote heterochromatin decondensation and subsequently allows DSB repair (26).

Finally, the identified synthetic lethality between ATR and dGcn5 mutant flies suggests that the correct functioning of the dGcn5-mediated DSB movement pathway is important to preserve genome stability. Since both ATR (25) and dGcn5 (this study) are required for proper movement of DSBs, we suggest that the decreased viability associated with the mutations in both proteins is due to the defective repair of heterochromatic DSBs. Although we cannot exclude that the synthetic lethality is caused by the contributions of dGcn5 to the recruitment of the SWI/SNF remodeling complex to DSBs (49,79), we did not observe defects in the γH2Av accumulation and resolution in euchromatin (Figure 2C), suggesting that euchromatic DSB repair can occur in the absence of dGcn5 in *Drosophila*.

Overall, our results provide an exciting illustration of how heterochromatin uniquely responds to a DSB and modifies its chromatin features to promote successful repair. This is in line with the idea that chromatin components and chromatin-associated factors actively participate in the process of DSB repair and are fine-tuned depending on the respective chromatin domain (31,46,80). Future research into how diverse chromatin environments affect and regulate the response to DSBs therefore represents a critical goal for understanding not only how genomic stability is maintained across the eukaryotic nucleus, but also how failure to maintain genomic integrity can result in disease development.

Data availability

The RNA-seq data underlying this article are available in NCBI GEO database and can be accessed with ID GSE262489.

Supplementary data

Supplementary Data are available at NAR Online.

Acknowledgements

We thank all the members of the Lens and Janssen labs for their valuable input during laboratory meetings. We acknowledge the Utrecht Sequencing Facility (USEQ) for providing sequencing service and data. Graphical abstract, Figure 5E and Figure 1A were created with Biorender.com.

Funding

European Research Council (ERC) under the European Union's Horizon 2020 research and innovation program [850405]; VIDI VI.Vidi.203.001 financed by the Dutch Research Council (NWO); USEQ is subsidized by the University Medical Center Utrecht and The Netherlands X-omics Initiative [NWO project 184.034.019]; G.H.K. and S.U.C. were supported by NIGMS of the US National Institutes of Health [R35GM139653].

Conflict of interest statement

None declared.

References

1. Barra,V. and Fachinetti,D. (2018) The dark side of centromeres: types, causes and consequences of structural abnormalities implicating centromeric DNA. *Nat. Commun.*, **9**, 4340.
2. Willis,N.A., Rass,E. and Scully,R. (2015) Deciphering the code of the cancer genome: mechanisms of chromosome rearrangement. *Trends Cancer*, **1**, 217–230.
3. Ramsden,D.A. and Nussenzweig,A. (2021) Mechanisms driving chromosomal translocations: lost in time and space. *Oncogene*, **40**, 4263–4270.
4. Roukos,V. and Misteli,T. (2014) The biogenesis of chromosome translocations. *Nat. Cell Biol.*, **16**, 293–300.
5. Ciccia,A. and Elledge,S.J. (2010) The DNA damage response: making it safe to play with knives. *Mol. Cell*, **40**, 179–204.
6. Scully,R., Panday,A., Elango,R. and Willis,N.A. (2019) DNA double-strand break repair-pathway choice in somatic mammalian cells. *Nat. Rev. Mol. Cell Biol.*, **20**, 698–714.
7. Hauer,M.H. and Gasser,S.M. (2017) Chromatin and nucleosome dynamics in DNA damage and repair. *Genes Dev.*, **31**, 2204–2221.
8. Hoskins,R.A., Carlson,J.W., Kennedy,C., Acevedo,D., Evans-Holm,M., Frise,E., Wan,K.H., Park,S., Mendez-Lago,M., Rossi,F., *et al.* (2007) Sequence finishing and mapping of drosophila melanogaster heterochromatin. *Science*, **316**, 1625–1628.
9. Padeken,J., Zeller,P. and Gasser,S.M. (2015) Repeat DNA in genome organization and stability. *Curr. Opin. Genet. Dev.*, **31**, 12–19.
10. Allshire,R.C. and Madhani,H.D. (2018) Ten principles of heterochromatin formation and function. *Nat. Rev. Mol. Cell Biol.*, **19**, 229–244.
11. Lachner,M., O'Carroll,D., Rea,S., Mechtler,K. and Jenuwein,T. (2001) Methylation of histone H3 lysine 9 creates a binding site for HP1 proteins. *Nature*, **410**, 116–120.
12. Bannister,A.J., Zegerman,P., Partridge,J.F., Miska,E.A., Thomas,J.O., Allshire,R.C. and Kouzarides,T. (2001) Selective recognition of methylated lysine 9 on histone H3 by the HP1 chromo domain. *Nature*, **410**, 120–124.
13. James,T.C. and Elgin,S.C. (1986) Identification of a nonhistone chromosomal protein associated with heterochromatin in Drosophila melanogaster and its gene. *Mol. Cell. Biol.*, **6**, 3862–3872.
14. Heitz,E. (1928) Das heterochromatin der Moose. *Jahrb Wiss Botanik*, **69**, 762–818.
15. Passarge,E. (1979) Emil Heitz and the concept of heterochromatin: longitudinal chromosome differentiation was recognized fifty years ago. *Am. J. Hum. Genet.*, **31**, 106–115.
16. Strom,A.R., Emelyanov,A.V., Mir,M., Fyodorov,D.V., Darzacq,X. and Karpen,G.H. (2017) Phase separation drives heterochromatin domain formation. *Nature*, **547**, 241–245.
17. Larson,A.G., Elnatan,D., Keenen,M.M., Trnka,M.J., Johnston,J.B., Burlingame,A.L., Agard,D.A., Redding,S. and Narlikar,G.J. (2017) Liquid droplet formation by HP1α suggests a role for phase separation in heterochromatin. *Nature*, **547**, 236–240.
18. Goodarzi,A.A., Noon,A.T., Deckbar,D., Ziv,Y., Shiloh,Y., Löbrich,M. and Jeggo,P.A. (2008) ATM signaling facilitates repair of DNA double-strand breaks associated with heterochromatin. *Mol. Cell*, **31**, 167–177.
19. Goodarzi,A.A., Kurka,T. and Jeggo,P.A. (2011) KAP-1 phosphorylation regulates CHD3 nucleosome remodeling during the DNA double-strand break response. *Nat. Struct. Mol. Biol.*, **18**, 831–839.
20. Noon,A.T., Shibata,A., Rief,N., Löbrich,M., Stewart,G.S., Jeggo,P.A. and Goodarzi,A.A. (2010) 53BP1-dependent robust localized KAP-1 phosphorylation is essential for heterochromatic DNA double-strand break repair. *Nat. Cell Biol.*, **12**, 177–184.
21. Garvin,A.J., Densham,R.M., Blair-Reid,S.A., Pratt,K.M., Stone,H.R., Weekes,D., Lawrence,K.J. and Morris,J.R. (2013) The deSUMOylase SENP7 promotes chromatin relaxation for homologous recombination DNA repair. *EMBO Rep.*, **14**, 975–983.
22. Ziv,Y., Bielopolski,D., Galanty,Y., Lukas,C., Taya,Y., Schultz,D.C., Lukas,J., Bekker-Jensen,S., Bartek,J. and Shiloh,Y. (2006) Chromatin relaxation in response to DNA double-strand breaks is modulated by a novel ATM- and KAP-1 dependent pathway. *Nat. Cell Biol.*, **8**, 870–876.
23. Klement,K., Luijsterburg,M.S., Pinder,J.B., Cena,C.S., Del Nero,V., Wintersinger,C.M., Dellaire,G., van Attikum,H. and Goodarzi,A.A. (2014) Opposing ISWI- and CHD-class chromatin remodeling activities orchestrate heterochromatic DNA repair. *J. Cell Biol.*, **207**, 717–733.
24. Sripathy,S.P., Stevens,J. and Schultz,D.C. (2006) The KAP1 corepressor functions to coordinate the assembly of de novo HP1-demarcated microenvironments of heterochromatin required for KRAB zinc finger protein-mediated transcriptional repression. *Mol. Cell. Biol.*, **26**, 8623–8638.
25. Chiolo,I., Minoda,A., Colmenares,S.U., Polyzos,A., Costes,S.V. and Karpen,G.H. (2011) Double-strand breaks in heterochromatin move outside of a dynamic HP1a domain to complete recombinational repair. *Cell*, **144**, 732–744.
26. Falk,M., Lukasova,E., Gabrielova,B., Ondrej,V. and Kozubek,S. (2007) Chromatin dynamics during DSB repair. *Biochim. Biophys. Acta*, **1773**, 1534–1545.
27. Jakob,B., Splinter,J., Conrad,S., Voss,K.-O., Zink,D., Durante,M., Löbrich,M. and Taucher-Scholz,G. (2011) DNA double-strand breaks in heterochromatin elicit fast repair protein recruitment, histone H2AX phosphorylation and relocation to euchromatin. *Nucleic Acids Res.*, **39**, 6489–6499.
28. Tsouroula,K., Furst,A., Rogier,M., Heyer,V., Maglott-Roth,A., Ferrand,A., Reina-San-Martin,B. and Soutoglou,E. (2016) Temporal and spatial uncoupling of DNA double strand break repair pathways within mammalian heterochromatin. *Mol. Cell*, **63**, 293–305.
29. Ryu,T., Spatola,B., Delabaere,L., Bowlin,K., Hopp,H., Kunitake,R., Karpen,G.H. and Chiolo,I. (2015) Heterochromatic breaks move to the nuclear periphery to continue recombinational repair. *Nat. Cell Biol.*, **17**, 1401–1411.
30. Janssen,A., Breuer,G.A., Brinkman,E.K., van der Meulen,A.I., Borden,S.V., van Steensel,B., Bindra,R.S., LaRocque,J.R. and

Karpen,G.H. (2016) A single double-strand break system reveals repair dynamics and mechanisms in heterochromatin and euchromatin. *Genes Dev.*, **30**, 1645–1657.
31. Kendek,A., Wensveen,M.R. and Janssen,A. (2021) The sound of silence: how silenced chromatin orchestrates the repair of double-strand breaks. *Genes*, **12**, 1415.
32. Ryu,T., Bonner,M.R. and Chiolo,I. (2016) Cervantes and Quijote protect heterochromatin from aberrant recombination and lead the way to the nuclear periphery. *Nucleus*, **7**, 485–497.
33. Uhlmann,F. (2016) SMC complexes: from DNA to chromosomes. *Nat. Rev. Mol. Cell Biol.*, **17**, 399–412.
34. Davidson,I.F. and Peters,J.-M. (2021) Genome folding through loop extrusion by SMC complexes. *Nat. Rev. Mol. Cell Biol.*, **22**, 445–464.
35. Pradhan,B., Kanno,T., Umeda Igarashi,M., Loke,M.S., Baaske,M.D., Wong,J.S.K., Jeppsson,K., Björkegren,C. and Kim,E. (2023) The Smc5/6 complex is a DNA loop-extruding motor. *Nature*, **616**, 843–848.
36. Jeppsson,K., Carlborg,K.K., Nakato,R., Berta,D.G., Lilienthal,I., Kanno,T., Lindqvist,A., Brink,M.C., Dantuma,N.P., Katou,Y., *et al.* (2014) The chromosomal association of the Smc5/6 complex depends on cohesion and predicts the level of sister chromatid entanglement. *PLoS Genet.*, **10**, e1004680.
37. Venegas,A.B., Natsume,T., Kanemaki,M. and Hickson,I.D. (2020) Inducible degradation of the Human SMC5/6 complex reveals an essential role only during interphase. *Cell Rep.*, **31**, 107533.
38. Potts,P.R. and Yu,H. (2007) The SMC5/6 complex maintains telomere length in ALT cancer cells through SUMOylation of telomere-binding proteins. *Nat. Struct. Mol. Biol.*, **14**, 581–590.
39. De Piccoli,G., Cortes-Ledesma,F., Ira,G., Torres-Rosell,J., Uhle,S., Farmer,S., Hwang,J.-Y., Machin,F., Ceschia,A., McAleenan,A., *et al.* (2006) Smc5-Smc6 mediate DNA double-strand-break repair by promoting sister-chromatid recombination. *Nat. Cell Biol.*, **8**, 1032–1034.
40. Potts,P.R., Porteus,M.H. and Yu,H. (2006) Human SMC5/6 complex promotes sister chromatid homologous recombination by recruiting the SMC1/3 cohesin complex to double-strand breaks. *EMBO J.*, **25**, 3377–3388.
41. Mahrik,L., Stefanovie,B., Maresova,A., Princova,J., Kolesar,P., Lelkes,E., Faux,C., Helmlinger,D., Prevorovsky,M. and Palecek,J.J. (2023) The SAGA histone acetyltransferase module targets SMC5/6 to specific genes. *Epigenetics Chromatin*, **16**, 6.
42. Díaz,M., Pečinková,P., Nowicka,A., Baroux,C., Sakamoto,T., Gandha,P.Y., Jeřábková,H., Matsunaga,S., Grossniklaus,U. and Pecinka,A. (2019) The SMC5/6 complex subunit NSE4A is involved in DNA damage repair and seed development. *Plant Cell*, **31**, 1579–1597.
43. Clouaire,T., Rocher,V., Lashgari,A., Arnould,C., Aguirrebengoa,M., Biernacka,A., Skrzypczak,M., Aymard,F., Fongang,B., Dojer,N., *et al.* (2018) Comprehensive mapping of histone modifications at DNA double-strand breaks deciphers repair pathway chromatin signatures. *Mol. Cell*, **72**, 250–262.
44. Clouaire,T. and Legube,G. (2019) A snapshot on the cis chromatin response to DNA double-strand breaks. *Trends Genet.*, **35**, 330–345.
45. Colmenares,S.U., Swenson,J.M., Langley,S.A., Kennedy,C., Costes,S.V. and Karpen,G.H. (2017) Drosophila histone demethylase KDM4A has enzymatic and non-enzymatic roles in controlling heterochromatin integrity. *Dev. Cell*, **42**, 156–169.
46. Janssen,A., Colmenares,S.U., Lee,T. and Karpen,G.H. (2019) Timely double-strand break repair and pathway choice in pericentromeric heterochromatin depend on the histone demethylase dKDM4A. *Genes Dev.*, **33**, 103–115.
47. Guo,R., Chen,J., Mitchell,D.L. and Johnson,D.G. (2011) GCN5 and E2F1 stimulate nucleotide excision repair by promoting H3K9 acetylation at sites of damage. *Nucleic Acids Res.*, **39**, 1390–1397.
48. Tjeertes,J.V., Miller,K.M. and Jackson,S.P. (2009) Screen for DNA-damage-responsive histone modifications identifies H3K9Ac and H3K56Ac in human cells. *EMBO J.*, **28**, 1878–1889.
49. Lee,H.-S., Park,J.-H., Kim,S.-J., Kwon,S.-J. and Kwon,J. (2010) A cooperative activation loop among SWI/SNF, gamma-H2AX and H3 acetylation for DNA double-strand break repair. *EMBO J.*, **29**, 1434–1445.
50. Tamburini,B.A. and Tyler,J.K. (2005) Localized histone acetylation and deacetylation triggered by the homologous recombination pathway of double-strand DNA repair. *Mol. Cell. Biol.*, **25**, 4903–4913.
51. Crona,F., Dahlberg,O., Lundberg,L.E., Larsson,J. and Mannervik,M. (2013) Gene regulation by the lysine demethylase KDM4A in Drosophila. *Dev. Biol.*, **373**, 453–463.
52. Jaklevic,B.R. and Su,T.T. (2004) Relative contribution of DNA repair, cell cycle checkpoints, and cell death to survival after DNA damage in Drosophila larvae. *Curr. Biol.*, **14**, 23–32.
53. Riddle,N.C., Minoda,A., Kharchenko,P.V., Alekseyenko,A.A., Schwartz,Y.B., Tolstorukov,M.Y., Gorchakov,A.A., Jaffe,J.D., Kennedy,C., Linder-Basso,D., *et al.* (2011) Plasticity in patterns of histone modifications and chromosomal proteins in Drosophila heterochromatin. *Genome Res.*, **21**, 147–163.
54. O'Geen,H., Echipare,L. and Farnham,P.J. (2011) Using ChIP-seq technology to generate high-resolution profiles of histone modifications. *Methods Mol. Biol.*, **791**, 265–286.
55. Ayrapetov,M.K., Gursoy-Yuzugullu,O., Xu,C., Xu,Y. and Price,B.D. (2014) DNA double-strand breaks promote methylation of histone H3 on lysine 9 and transient formation of repressive chromatin. *Proc. Natl. Acad. Sci. U.S.A.*, **111**, 9169–9174.
56. Feller,C., Forné,I., Imhof,A. and Becker,P.B. (2015) Global and specific responses of the histone acetylome to systematic perturbation. *Mol. Cell*, **57**, 559–571.
57. Karam,C.S., Kellner,W.A., Takenaka,N., Clemmons,A.W. and Corces,V.G. (2010) 14-3-3 mediates histone cross-talk during transcription elongation in Drosophila. *PLoS Genet.*, **6**, e1000975.
58. Carré,C., Szymczak,D., Pidoux,J. and Antoniewski,C. (2005) The histone H3 acetylase dGcn5 is a key player in Drosophila melanogaster metamorphosis. *Mol. Cell. Biol.*, **25**, 8228–8238.
59. Vamos,E.E. and Boros,I.M. (2012) The C-terminal domains of ADA2 proteins determine selective incorporation into GCN5-containing complexes that target histone H3 or H4 for acetylation. *FEBS Lett.*, **586**, 3279–3286.
60. Ciabrelli,F., Rabbani,L., Cardamone,F., Zenk,F., Löser,E., Schächtle,M.A., Mazina,M., Loubiere,V. and Iovino,N. (2023) CBP and Gcn5 drive zygotic genome activation independently of their catalytic activity. *Sci. Adv.*, **9**, eadf2687.
61. Yu,D., Tan,Y., Chakraborty,M., Tomchik,S. and Davis,R.L. (2018) Elongator complex is required for long-term olfactory memory formation in Drosophila. *Learn. Mem.*, **25**, 183–196.
62. Eissenberg,J.C. and Reuter,G. (2009) Chapter 1 cellular mechanism for targeting heterochromatin formation in Drosophila. *Int. Rev. Cell Mol. Biol.* **273**, 1–47.
63. Zou,L. and Elledge,S.J. (2003) Sensing DNA damage through ATRIP recognition of RPA-ssDNA complexes. *Science*, **300**, 1542–1548.
64. Ciurciu,A., Komonyi,O., Pankotai,T. and Boros,I.M. (2006) The drosophila histone acetyltransferase Gcn5 and transcriptional adaptor Ada2a are involved in nucleosomal histone H4 acetylation. *Mol. Cell. Biol.*, **26**, 9413–9423.
65. Sancar,A., Lindsey-Boltz,L.A., Unsal-Kaçmaz,K. and Linn,S. (2004) Molecular mechanisms of mammalian DNA repair and the DNA damage checkpoints. *Annu. Rev. Biochem.*, **73**, 39–85.
66. Laurençon,A., Purdy,A., Sekelsky,J., Hawley,R.S. and Su,T.T. (2003) Phenotypic analysis of separation-of-function alleles of MEI-41, Drosophila ATM/ATR. *Genetics*, **164**, 589–601.
67. Falk,M. and Hausmann,M. (2020) A paradigm revolution or just better resolution-will newly emerging superresolution techniques identify chromatin architecture as a key factor in radiation-induced DNA damage and repair regulation? *Cancers (Basel)*, **13**, 18.
68. Schep,R., Brinkman,E.K., Leemans,C., Vergara,X., van der Weide,R.H., Morris,B., van Schaik,T., Manzo,S.G.,

Peric-Hupkes,D., van den Berg,J., *et al.* (2021) Impact of chromatin context on Cas9-induced DNA double-strand break repair pathway balance. *Mol. Cell*, **81**, 2216–2230.
69. Vergara,X., Manjón,A.G., de Haas,M., Morris,B., Schep,R., Leemans,C., Friskes,A., Beijersbergen,R.L., Sanders,M.A., Medema,R.H., *et al.* (2024) Widespread chromatin context-dependencies of DNA double-strand break repair proteins. *Nat. Commun.*, **15**, 5334.
70. Brand,M., Moggs,J.G., Oulad-Abdelghani,M., Lejeune,F., Dilworth,F.J., Stevenin,J., Almouzni,G. and Tora,L. (2001) UV-damaged DNA-binding protein in the TFTC complex links DNA damage recognition to nucleosome acetylation. *EMBO J.*, **20**, 3187–3196.
71. Dhalluin,C., Carlson,J.E., Zeng,L., He,C., Aggarwal,A.K. and Zhou,M.M. (1999) Structure and ligand of a histone acetyltransferase bromodomain. *Nature*, **399**, 491–496.
72. Pai,C.-C., Deegan,R.S., Subramanian,L., Gal,C., Sarkar,S., Blaikley,E.J., Walker,C., Hulme,L., Bernhard,E., Codlin,S., *et al.* (2014) A histone H3K36 chromatin switch coordinates DNA double-strand break repair pathway choice. *Nat. Commun.*, **5**, 4091.
73. Espinosa,M.C., Rehman,M.A., Chisamore-Robert,P., Jeffery,D. and Yankulov,K. (2010) GCN5 is a positive regulator of origins of DNA replication in Saccharomyces cerevisiae. *PLoS One*, **5**, e8964.
74. Otterstrom,J., Castells-Garcia,A., Vicario,C., Gomez-Garcia,P.A., Cosma,M.P. and Lakadamyali,M. (2019) Super-resolution microscopy reveals how histone tail acetylation affects DNA compaction within nucleosomes in vivo. *Nucleic Acids Res.*, **47**, 8470–8484.
75. Yin,H., Sweeney,S., Raha,D., Snyder,M. and Lin,H. (2011) A high-resolution whole-genome map of key chromatin modifications in the adult Drosophila melanogaster. *PLoS Genet.*, **7**, e1002380.
76. Xu,J., Ma,H., Jin,J., Uttam,S., Fu,R., Huang,Y. and Liu,Y. (2018) Super-resolution imaging of higher-order chromatin structures at different epigenomic states in single mammalian cells. *Cell Rep.*, **24**, 873–882.
77. Gibson,B.A., Doolittle,L.K., Schneider,M.W.G., Jensen,L.E., Gamarra,N., Henry,L., Gerlich,D.W., Redding,S. and Rosen,M.K. (2019) Organization of chromatin by intrinsic and regulated phase separation. *Cell*, **179**, 470–484.
78. Caridi,C.P., D'Agostino,C., Ryu,T., Zapotoczny,G., Delabaere,L., Li,X., Khodaverdian,V.Y., Amaral,N., Lin,E., Rau,A.R., *et al.* (2018) Nuclear F-actin and myosins drive relocalization of heterochromatic breaks. *Nature*, **559**, 54–60.
79. Bennett,G. and Peterson,C.L. (2015) SWI/SNF recruitment to a DNA double-strand break by the NuA4 and Gcn5 histone acetyltransferases. *DNA Repair (Amst.)*, **30**, 38–45.
80. Clouaire,T. and Legube,G. (2015) DNA double strand break repair pathway choice: a chromatin based decision?*Nucleus*, **6**, 107–113.

Received: March 26, 2024. **Revised:** August 20, 2024. **Editorial Decision:** August 22, 2024. **Accepted:** August 26, 2024